

Photometric Solutions of Some Contact ASAS Binaries

İ.Gezer^{1*}, Z. Bozkurt¹

¹*Astronomy and Space Science Department, Ege University, 35100 Bornova, Izmir, Turkey*

Abstract

We present the first light curve solution of 6 contact binary systems which are chosen from the ASAS catalog. The photometric elements and the estimated absolute parameters of all systems are obtained with the light curve analyses. We calculated the values of degree of contact for the systems. The location of the targets on the Hertzsprung–Russell diagram and the mass–radius plane is compared to the other well-known contact binaries and the evolutionary status of the systems are also discussed.

Keywords: stars: binaries: eclipsing — stars: fundamental parameters — stars: low-mass — stars: individual: (ASAS 002821-1453.3, ASAS 012450-3241.4, ASAS 024155-2507.8, ASAS 050334-2521.9, ASAS 051353-1701.2, ASAS 063546+1928.6)

1. Introduction

ASAS (All Sky Automated Survey, (Pojmanski, 1997)) is a project which aims to detect any kind of photometric variability by monitoring the large area of the sky with fully automated instruments. One of the main objec-

*Corresponding author
E-mail address: gezer.ilknur@gmail.com

tives of ASAS is to find and catalog variable stars. Through the project, approximately 10^7 stars which are brighter than 14^m have been observed so far. The prototype of the project was first operated in 1996 at the Warsaw University Astronomical Observatory. Now, it carries on with three full automatic instruments having V and I filters attached to CCD cameras at Las Campanas Observatory in Chile and at Mt. Haleakala Observatory in Maui, Hawaii. The categorized stars are relatively located in the southern hemisphere ($\delta < +28^\circ$) and many of them are newly discovered. The public domain data of the ASAS also ease the achievement and investigation of the systems in detail. ASAS apparent magnitudes were transformed into the standard 'I' and 'V' systems using Landolt (1992) and Hipparcos Perryman et al. (1997). The photometric accuracy is given about 0.05 mag in most cases.

Pojmanski (2000) published the first results of observations obtained by the prototype ASAS camera and gave a catalog containing 3800 variable stars. According to Paczyński et al. (2006) 11076 eclipsing binaries (including 5384 contact systems) were discovered. They presented the preliminary results of the analysis for thousands of binary systems. They also emphasized that their statistical investigation supports the hypothesis in which the thermal relaxation oscillation states of contact binaries (Flannery, 1976; Lucy, 1976).

The targets in our study were selected from the eclipsing binary list of Paczyński et al. (2006). We chose our targets according to the criteria that no detailed investigation can be found in literature. The main properties of the targets are listed in Table 1. In the next section we present the

Table 1: Properties of the selected targets. RA, DEC and T_0 refer to the right ascension, the declination and the time of minimum light, respectively. V_{max} and V_{amp} denote the maximum brightness and the amplitude of variation in V filter.

ASAS Number	Other ID	RA(^h ^m ^s)	DEC(^o ^m ^s)	T_0 (HJD-2450000)	Period(^d)	$V_{max}^{(m)}$	$V_{amp}^{(m)}$
002821-1453.3	TYC 5268-1013-1	00 28 21	-14 53 18	1869.060	0.402660	11.54	0.44
012450-3241.4	TYC 7002-320-1	01 24 50	-32 41 24	1869.099	0.308971	11.45	0.58
024155+2507.8	TYC 1772-674-1	02 41 55	25 07 48	2621.660	0.400889	11.73	0.61
050334-2521.9	TYC 6477-224-1	05 03 34	-25 21 54	1868.980	0.414060	11.09	0.31
051353-1701.2	TYC 5906-87-1	05 13 53	-17 01 12	1869.140	0.341836	11.66	0.55
063546+1928.6	TYC 1337-1137-1	06 35 46	19 28 36	2621.780	0.475511	9.95	0.43

temperature determination method for primary components and the details of the light curve analyses. In section 3, we give detailed information about the targets and some crucial parameters obtained by the light curve solutions. We conclude the results and compare the evolutionary status of the targets to known contact binaries in the last section.

2. Light curve analyses of programme stars

2.1. Temperature determination

Since the light curve analysis of an eclipsing binary system requires the effective temperature of at least one of the components, the accurate determination of the effective temperature is a critical step in the solution. Our program stars do not have any detailed spectroscopic or photometric study in the literature, however, their Johnson, 2MASS and Tycho magnitudes are given in several data archives. In this case the only way to determine their temperature is to use different colors and temperature calibrations. We used

Table 2: The extinction ratios of different photometric systems given by (Ramírez & Meléndez, 2005)

Color	Photometric system	k^a
$(V - J_2)$	Johnson-2MASS	2.16
$(V - H_2)$	Johnson-2MASS	2.51
$(V - K_2)$	Johnson-2MASS	2.70
$(B_T - V_T)$	Tycho	1.02
$(V_T - K_2)$	Tycho-2MASS	2.87

$$^a k = E(\text{color}) / E(B-V)$$

the calibrations given by Ramírez & Meléndez (2005) who listed the adopted extinction ratios for various photometric systems. For the reddening correction, we used calibrations given in Table 2 (Ramírez & Meléndez, 2005) and $E(B - V)$ values which are obtained from Kurucz models (Castelli & Kurucz, 2003). The $(V - K)$ color was decided to use in the light curve solution because of its relatively low dependence on the metallicity. We then determined the effective temperatures of primary components for derived intrinsic colour indices by using the appropriate table (Table 11) of Ramírez & Meléndez (2005). During our calculations, we assumed that the primary component is a main-sequence star and its metallicity value is equal to solar metallicity, $[\text{Fe}/\text{H}] = +0.0$. Finally, the average values of two calculated temperatures corresponding to $(V - K_2)$ and $(V_T - K_2)$ colors of each target adopted as the effective temperature values for primary components.

2.2. Analyses

The V -band light curves of selected contact binary systems were collected from the ASAS database. We analysed all light curves by using the PHOEBE Prša & Zwitter (2005) software, which is based on the Wilson–Devinney code Wilson & Devinney (1971). The unmeasured and grade D (noted as useless) data were not included to our analyses. The gravitational darkening coefficients of the primary and secondary components, g_1 and g_2 , were chosen from Ruciński (1969) while the albedo values, A_1 and A_2 , were taken from van Hamme (1993). The following parameters were set as adjustable during the light curve analysis: The inclination of the orbit, i , mass ratio $q = M_2/M_1$, temperature of the secondary component, T_2 , dimensionless surface potentials of the primary and secondary components, $\Omega_1 = \Omega_2$, unnormalized monochromatic luminosity of the primary component, L_1 , the time of primary minimum, T_0 , and the orbital period of the binary, P . Additionally, we calculated the fillout factor of each system by using the following equation (Lucy & Wilson, 1979),

$$f = \frac{\Omega_i - \Omega}{\Omega_i - \Omega_o}, \quad (1)$$

where Ω_i is the inner and Ω_o is the outer Lagrangian potentials. As a first step, we tried to find a solution for all light curves including all observational points (including those with large scattered ones) from the ASAS database. When we reach a reasonable solution, we calculated the differences between the theoretical and observational light curves points for this initial solution. In order to extract the useless scattered points we calculated the standard deviations, σ , of these differences and we removed the points located be-

yond the 3σ . Then we run the code again to find the final solution. The resulting parameters yielded by analysis of 6 systems including output errors of PHOEBE code are presented in Table 3 and the theoretical light curves among the observational points are also shown in Fig. 1. At the bottom of the figures we also present the differences between computed and observational light curves in the final solution. In the following subsections, we give the some details of the systems based on our analyses.

3. Individual objects

3.1. *ASAS 002821-1453.3*

According to our V light curve solution this system contains two components with temperature difference of about 50 K. Its light curve presents a typical W UMa type shape. $(V - K_2) = 1.0293$ and $(V_T - K_2) = 1.1072$ colors correspond to the effective temperatures of 6566 K and 6514 K, respectively. The fillout factor of the system is about 40%.

3.2. *ASAS 012450-3241.4*

The target is the coolest system among our selected binaries. Its $(V - K_2) = 1.9160$ and $(V_T - K_2) = 2.0320$ colors indicate a primary having $T = 5203$ K and $T = 5169$ K, respectively, according to our calculations. The results of our analysis show that temperature difference of the binary components is very small (~ 22 K) and one can assume that the two companions have almost equal effective temperature values. Its fillout factor is about 13%.

Table 3: Results of the light curve analysis of the systems. Formal error estimates are given in parenthesis.

Parameter	002821-1453.3	012450-3241.4	024155+2507.8
i ($^\circ$)	78.2(6)	81.8(6)	80.8(3)
q	0.173(7)	0.377(8)	0.45(1)
T_1 (K)	6540	5186	5746
T_2 (K)	6593(79)	5164(25)	5537(61)
$\Omega_1 = \Omega_2$	2.12(2)	2.60(2)	2.76(3)
f (%)	40	13	7
$\frac{L_1}{L_1+L_2}$	0.82(1)	0.71(1)	0.72(2)
$\overline{r_1}$	0.549(9)	0.472(7)	0.44(1)
$\overline{r_2}$	0.26(3)	0.30(1)	0.31(2)
T_0 (HJD-2450000)	2080.8634(6)	4740.6713(2)	4409.6264(6)
P (d)	0.4026640(1)	0.30897005(2)	0.40088802(5)
	050334-2521.9	051353-1701.2	063546-1928.6
i ($^\circ$)	83.3(2)	70.3(7)	85.4(1)
q	0.133(3)	0.52(4)	0.173(4)
T_1 (K)	6347	5419	6229
T_2 (K)	5925(40)	5086(53)	6072(29)
$\Omega_1 = \Omega_2$	2.01(1)	2.81(8)	2.10(1)
f (%)	53	34	58
$\frac{L_1}{L_1+L_2}$	0.885(5)	0.71(3)	0.834(4)
$\overline{r_1}$	0.572(5)	0.46(3)	0.557(4)
$\overline{r_2}$	0.24(3)	0.35(4)	0.27(2)
T_0 (HJD-2450000)	3630.8372(4)	1914.6192(5)	3705.7085(3)
P (d)	0.41406990(4)	0.34183617(8)	0.47551487(3)

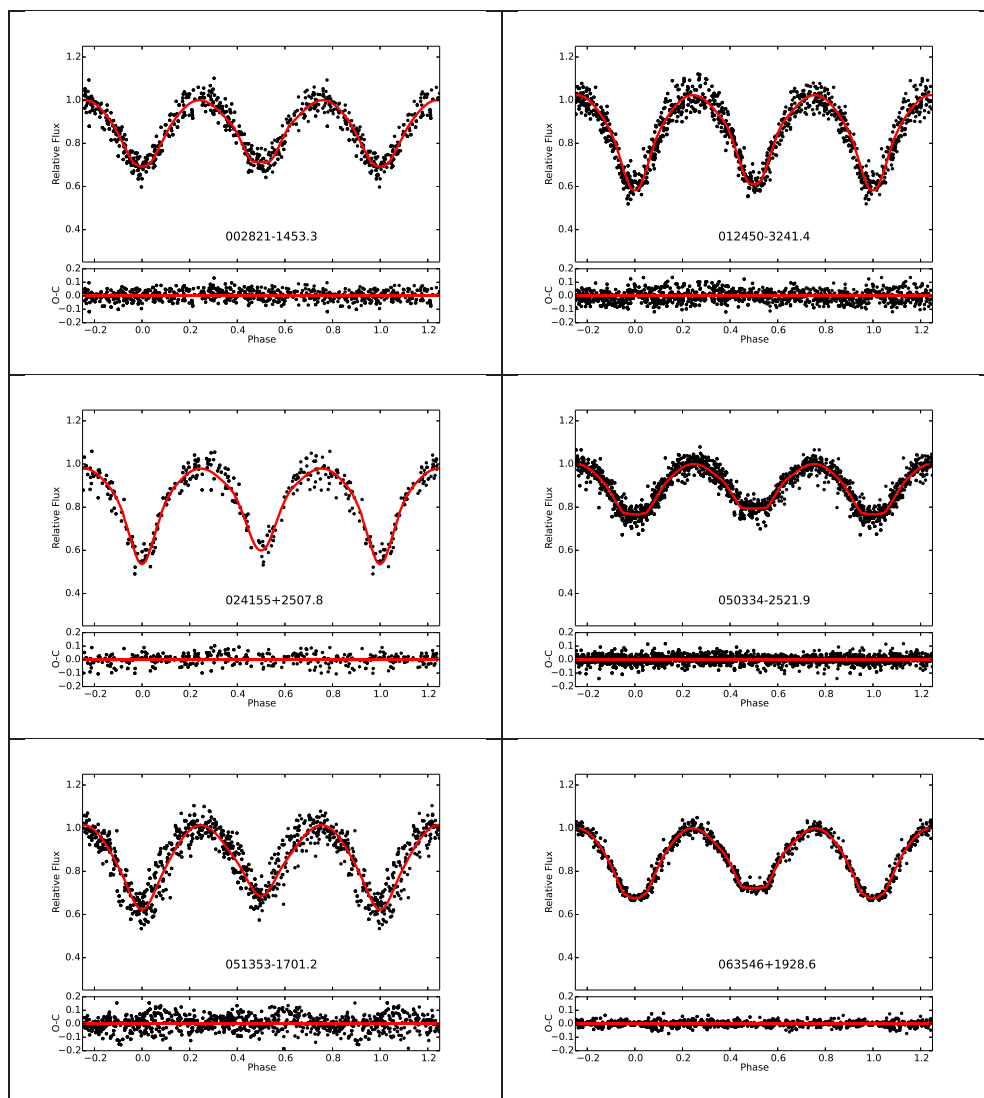


Figure 1: Agreement between the observational and calculated light curves. Dots indicate observations and lines refer theoretical curves. The ASAS number of the systems are written on the figures. At the bottom of each figure the differences between observational and calculated light curves are also shown.

3.3. ASAS 24155+2507.8

The system has the smallest fillout factor among our targets with the value of 7%. The temperature difference of two components is about 200 K. $(V - K_2) = 1.5122$ and $(V_T - K_2) = 1.5861$ colors correspond to the temperatures $T=5750$ K and $T=5746$ K, respectively.

3.4. ASAS 050334-2521.9

The target appeared in the catalog of Gettel, Geske & McKay (2006) with the orbital period value of 0.414075 days. Results of our analysis indicate that the system has a mass-ratio value of 0.133 and it can be put into a small group of deep, low mass-ratio contact binaries following the criteria of $f \geq 50\%$ given by Qian et al. (2005). Its $(V - K_2) = 1.1676$ and $(V_T - K_2) = 1.1945$ color values show that temperature of primary component is $T=6330$ K and $T = 6364$ K, respectively. There is a ~ 400 K temperature difference between the components of the binary system.

3.5. ASAS 51353+1701.2

$(V - K_2)$ and $(V_T - K_2)$ colors of this system are 1.7336 and 1.8333, and the temperatures corresponding these values are $T=5433$ K and $T = 5405$ K, respectively. It has the largest mass-ratio with its value of 0.52 among our selected targets. The temperature difference of two components and its fillout factor are about 350 K and 34%, respectively.

3.6. ASAS 063546+1928.6

The light curve of the system shows total eclipses and therefore has two flat bottomed minimums. The system's inclination, $85^\circ.4$, is the highest

Table 4: Estimated absolute parameters of the systems.

ASAS Number	M_1 (M_\odot)	M_2 (M_\odot)	R_1 (R_\odot)	R_2 (R_\odot)	T_1 (K)	T_2 (K)	L_1 (L_\odot)	L_2 (L_\odot)
002821-1453.3	1.33	0.230(9)	1.49(2)	0.60(2)	6540	6593(79)	3.7(1)	0.70(4)
012450-3241.4	0.79	0.298(6)	0.96(1)	0.58(3)	5186	5164(25)	0.59(2)	0.21(3)
024155+2507.8	0.97	0.430(1)	1.18(3)	0.77(7)	5746	5537(61)	1.37(7)	0.50(9)
050334-2521.9	1.26	0.168(4)	1.54(1)	0.60(1)	6347	5925(40)	3.45(6)	0.40(2)
051353-1701.2	0.89	0.460(4)	1.07(7)	0.80(1)	5419	5086(53)	0.90(1)	0.30(1)
063546+1928.6	1.19	0.206(5)	1.63(1)	0.70(1)	6229	6079(29)	3.60(6)	0.60(2)

among our targets. The star can be put into the group of deep, low mass–ratio contact binaries (Qian et al., 2005) owing to its degree of contact and mass–ratio values ($f=58\%$, $q=0.173$). ($V - K_2$) = 1.2140 and ($V_T - K_2$) = 1.2846 colors correspond to the temperatures $T=6247$ K and $T=6212$ K, respectively, and the temperature difference of two components is about 150 K.

4. Conclusions

We presented the first light curve solutions of six contact binaries selected from ASAS database. The initial parameters for temperatures during the analyses were chosen using the $V - K$ colors of the targets. The light parameters and the agreement between observations and analysis were also presented. The absolute parameters were determined by estimating the masses of the primary components using the correlation given by Cox (2000). These parameters are listed in Table 4. The calculation of the degree of contact (f) for all systems indicates that our targets cover a large interval of this parameter (7-58%).

The contact binary stars were divided into two subclasses, A– and W–

types, by Binnendijk (1970). The author mentioned that A-type contacts have the hotter components which are occulted during the primary minimum while W-types are the systems where the hotter companions are the less massive ones. According to this criteria, all of our targets belong to A-type.

Lucy (1968) proposed that contact binary systems have two components sharing common envelope whose temperature is nearly constant through the surface. Thermal relaxation oscillations are the cyclic mass transfer phases that are suggested for the evolution of the contact binaries (Flannery, 1976; Lucy, 1976) although there are studies contrary to this idea. Paczyński et al. (2006) mentioned that the controversy probably rises from the binary systems having the period between $0.3 < P < 1.2$ days and are not in thermal contact. A- and W-type subclasses were thought to have different evolutionary properties for a long time. Maceroni & van't Veer (1996), on the other hand, proposed three subclasses for contact binaries. According to their classification one group has hot components while the other groups, old and young late types, are characteristic W UMa systems. Later, Gazeas & Stępień (2008) advised that intermediate mass W-type systems evolve to high mass ratio A-type systems. They also concluded that the old and young late type contact binaries preserves their configuration in their whole phases of evolution. Stępień & Gazeas (2012) also suggested a scenario for cool contact binaries: the detached binaries having orbital period smaller than 2 days evolve to a system transferring mass from the more massive component to less massive one and then to a contact binary. The evolution finalizes with the merging process which produces a rapidly rotating single star. We compared the results of the analyses for our targets with the well known contact binaries.

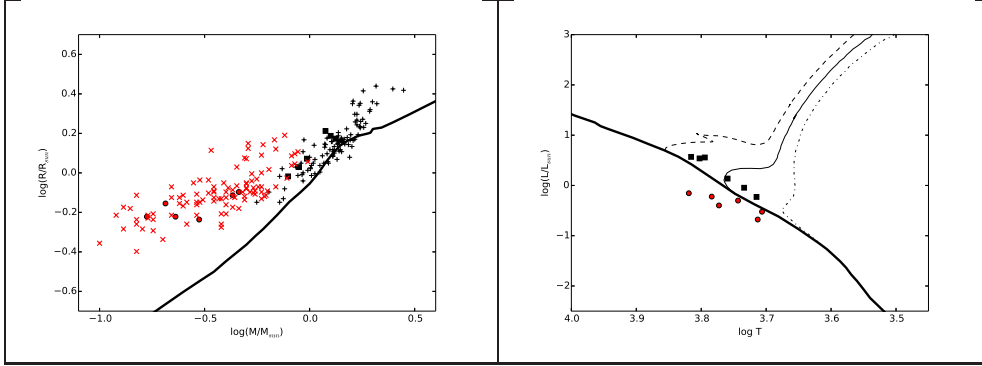


Figure 2: The locations of the targets on mass–radius plane (left) and Hertzsprung–Russell diagram (right). The squares (black in coloured edition) indicate the primary components while the filled circles (red in coloured edition) denote the secondaries of our targets. The plus (black in coloured edition) and cross signs (red in coloured edition) on mass–radius plane correspond to primary and secondary components of contact binaries collected from Yıldız & Doğan (2013). The thick solid lines indicate the zero age main sequence (ZAMS). The dashed, thin solid and dot–dashed lines show the evolutionary tracks of the stars having the initial mass of $1.5M_{\odot}$, $1M_{\odot}$ and $0.6M_{\odot}$. The data for ZAMS and the evolutionary tracks are taken from Girardi et al. (2000).

To make this comparison, we located the systems on mass–radius plane together with 100 contact binaries whose physical parameters were given by Yıldız & Doğan (2013). Fig. 2 shows the locations of our targets together with the other contact binaries. The primary and secondary components are gathered in two separate regions in an accordance with other contact binaries. Therefore, our targets are in good agreement with other contact binaries in the plane. The positions of the components of the targets on the Hertzsprung–Russell diagram are also plotted in Fig. 2. The secondaries are generally seen slightly under the main sequence while the primaries are on it as hypothesize. The evolutionary status of our targets shows that primary components of some of our targets seem more evolved than other ones which can be seen by the help of the evolutionary tracks drawn for the stars having the initial mass of $1.5M_{\odot}$, $1M_{\odot}$ and $0.6M_{\odot}$ on the Hertzsprung–Russell diagram.

Acknowledgements

This research has made use of the SIMBAD (operated at CDS, Strasbourg, France) database. Besides the ASAS catalogue, 2MASS and Tycho catalogues also helped us to determine the colors of our targets.

References

Bernhard K., 2004, BAVSR, 53, 108

Binnendijk L., 1970, VA, 12, 217

Cox A. N., 2000, asqu.book

de Geus E. J., Lub J., van de Grift E., 1990, A&AS, 85, 915

Flannery B. P., 1976, ApJ, 205, 217

Flower P. J., 1996, ApJ, 469, 355

Gazeas K., Stępień K., 2008, MNRAS, 390, 1577

Gettel S. J., Geske M. T., McKay T. A., 2006, AJ, 131, 621

Girardi L., Bressan A., Bertelli G., Chiosi C., 2000, A&AS, 141, 371

Hoffman D. I., Harrison T. E., McNamara B. J., 2009, AJ, 138, 466

Kazarovets E. V., Samus N. N., Durlevich O. V., Kireeva N. N., Pastukhova E. N., 2011, IBVS, 5969, 1

Castelli F., Kurucz R. L., 2003, IAUS, 210, 20P

Koch R. H., Wood F. B., Florkowski D. R., Oliver J. P., 1979, IBVS, 1708, 1

Kozłowski S. K., Konacki M., Sybilski P., 2011, MNRAS, 416, 2020

Landolt, A. U., 1992, AJ, 104, 340

Lopez C. E., Girard T. M., 1990, PASP, 102, 1018

Lucy L. B., 1968, ApJ, 151, 1123

Lucy L. B., 1976, ApJ, 205, 208

Lucy L. B., Wilson R. E., 1979, ApJ, 231, 502

Maceroni C., van't Veer F., 1996, A&A, 311, 523

Malkov O. Y., Oblak E., Snegireva E. A., Torra J., 2006, *A&A*, 446, 785

Marraco L. G., Orsatti A. M., 1982, *RMxAA*, 5, 183

Muzzio J. C., Orsatti A. M., 1977, *AJ*, 82, 345

Paczyński B., Szczygieł D. M., Pilecki B., Pojmański G., 2006, *MNRAS*, 368, 1311

Perryman, M. A. C., Perryman, M. A. C., Kovalevsky, J., Hoeg, E., Bastian, U. and 15 coauthors, 1997, *A&A*, 323L, 49P

Philip A. G. D., Stock J., 1972, *BOTT*, 6, 201

Pojmanski G., 1997, *AcA*, 47, 467

Pojmanski G., 2000, *AcA*, 50, 177

Pols O. R., Tout C. A., Eggleton P. P., Han Z., 1995, *MNRAS*, 274, 964

Popova M., Kraicheva Z., 1984, *AISAO*, 18, 6

Prša A., Zwitter T., 2005, *ApJ*, 628, 426

Qian S.-B., Yang Y.-G., Soonthornthum B., Zhu L.-Y., He J.-J., Yuan J.-Z., 2005, *AJ*, 130, 224

Ramírez, I., Meléndez, J., 2005, *ApJ*, 626, 465

Ruciński S. M., 1969, *AcA*, 19, 245

Stępień K., Gazeas K., 2012, *AcA*, 62, 153

van Hamme W., 1993, *AJ*, 106, 2096

Wenger M., Ochsenbein, F., Egret, D., Dubois, P., Bonnarel, F. and 6 coauthors, 2000, *A&AS*, 143, 9

Wilson R. E., Devinney E. J., 1971, *ApJ*, 166, 605

Yıldız M., Doğan T., 2013, *MNRAS*, 430, 2029

This figure "HR.png" is available in "png" format from:

<http://arxiv.org/ps/1510.01045v1>

This figure "MR.png" is available in "png" format from:

<http://arxiv.org/ps/1510.01045v1>

This figure "n002821.png" is available in "png" format from:

<http://arxiv.org/ps/1510.01045v1>

This figure "n012450.png" is available in "png" format from:

<http://arxiv.org/ps/1510.01045v1>

This figure "n024155.png" is available in "png" format from:

<http://arxiv.org/ps/1510.01045v1>

This figure "n050334.png" is available in "png" format from:

<http://arxiv.org/ps/1510.01045v1>

This figure "n051353.png" is available in "png" format from:

<http://arxiv.org/ps/1510.01045v1>

This figure "n063546.png" is available in "png" format from:

<http://arxiv.org/ps/1510.01045v1>